Two-Channel Kondo Physics in Two-Impurity Kondo Models

Andrew K. Mitchell,[1] Eran Sela,[1] and David E. Logan[2]

[1]*Institute for Theoretical Physics, University of Cologne, 50937 Cologne, Germany*
[2]*Department of Chemistry, Physical and Theoretical Chemistry, Oxford University, South Parks Road, Oxford OX1 3QZ, United Kingdom*

(Received 26 November 2011; published 24 February 2012)

We consider the non-Fermi-liquid quantum critical state of the spin-S two-impurity Kondo model and its potential realization in a quantum dot device. Using conformal field theory and the numerical renormalization group, we show the critical point to be identical to that of the two-channel Kondo model with additional potential scattering, for any spin S. Distinct conductance signatures are shown to arise as a function of device asymmetry, with the square-root behavior commonly believed to arise at low-energies dominant only in certain regimes.

DOI: 10.1103/PhysRevLett.108.086405 PACS numbers: 71.10.Hf, 73.21.La, 73.63.Kv

Systems comprising several quantum impurities inherently display an interplay between impurity-bath and interimpurity couplings [1–7]: the tendency for impurities to be Kondo screened by conduction electrons competes with screening by interimpurity spin-singlet formation. Rich physics can thereby arise, as demonstrated, for example, in coupled quantum dots [7,8], magnetic impurities in metals [1], and recent two-impurity STM experiments [9]. Indeed, the same essential physics governs the analogous propensities for heavy fermion behavior or magnetic ordering in lattice systems [10].

The two-impurity, spin-$\frac{1}{2}$ Kondo model (2IKM) is the simplest to capture this competition [1]: local singlet formation is favored by an interimpurity exchange K, while coupling of each impurity to its own conduction channel favors separate Kondo screening below an effective single-channel, single-impurity scale T_K [2–5]. The lack of interchannel charge transfer in the 2IKM permits two distinct phases, and a quantum phase transition (QPT) results on tuning $K_c \sim T_K$. At the critical point, non-Fermi-liquid (NFL) physics arises below T_c, characterized [3] by anomalous properties such as fractional residual entropy and singular magnetic susceptibility.

This critical physics is also surprisingly robust to some perturbations, notably breaking of mirror (parity) symmetry or particle-hole symmetry [6]. Such perturbations are marginally irrelevant in the sense that the interimpurity coupling can be retuned to recover the critical point in all cases. But despite considerable effort, 2IKM critical physics has proved experimentally elusive—mainly due to interchannel charge transfer which smooths the QPT into a crossover [4]. Regular Fermi liquid (FL) physics then sets in below an energy scale T^*, and if the degree of charge transfer is large enough that $T^* \gg T_c$, no evidence of the critical point will be observed [11]. This is the situation relevant to the recent two-impurity experiments of Ref. [9]: coupling between one impurity on a metal surface and one on a STM tip was also accompanied by strong tip-surface tunneling.

Reducing the degree of interchannel charge transfer might be possible in a quantum dot device such as that proposed in Ref. [6]. Provided $T^* \ll T_c$, NFL behavior should be observable in an intermediate energy window, as can be understood from a 2IKM critical perspective (indeed the eventual crossover to FL physics is wholly characteristic of the intermediate NFL state [12]).

An alternative route could, however, involve use of a quantum box, which acts as an interacting lead [13]. Coupling a single dot to one regular lead and one box tuned to the Coulomb blockade regime suppresses interchannel charge transfer completely. This has been exploited to access single-impurity two-channel Kondo (2CK) physics [14,15] in a real device [13]. Here we propose simply to interject a second dot in series between the "leads" to realize 2IKM physics. While parity and particle-hole symmetries are thereby broken, the QPT itself is unaffected. Robust NFL behavior should persist down to the lowest energy scales at the critical point.

Here we address two key questions in regard to potential realization of 2IKM physics. First, what is the nature of the critical point itself? We show that it is *identical* to that arising in a 2CK model with additional potential scattering, *independent* of parity breaking. Further, we show that the same QPT and 2CK critical point arises in the spin-S generalization of the 2IKM. Second, what are the signatures of criticality in measurable quantities such as conductance? These reflect renormalization group (RG) flow from higher-energy fixed points (FPs) and depend sensitively on parity breaking. We find, in particular, that the square-root behavior commonly anticipated [6,7] at low energies is absent in the standard channel-symmetric 2IKM.

Nature of 2IKM critical point.—The 2IKM reads:

$$H_{\mathrm{2IKM}} = H_0 + H_{\mathrm{ps}} + J_L \vec{S}_L \cdot \vec{s}_{0L} + J_R \vec{S}_R \cdot \vec{s}_{0R} + K \vec{S}_L \cdot \vec{S}_R, \tag{1}$$

where $H_0 = \sum_{\alpha,k} \epsilon_k \psi^\dagger_{k\sigma\alpha} \psi_{k\sigma\alpha}$ describes two free conduction channels $\alpha = L/R$, with density of states ρ, and spin density at the impurities $\vec{s}_{0\alpha} = \sum_{\sigma\sigma'} \psi^\dagger_{0\sigma\alpha} (\frac{1}{2}\vec{\sigma}_{\sigma\sigma'}) \psi_{0\sigma'\alpha}$ (where $\psi^\dagger_{0\sigma\alpha} = \sum_k \psi^\dagger_{k\sigma\alpha}$). Potential scattering is included via $H_{\rm ps} = \sum_\alpha V_\alpha \psi^\dagger_{0\sigma\alpha} \psi_{0\sigma\alpha}$, and $\vec{S}_\alpha$ are spin-$\frac{1}{2}$ operators for the impurities. The 2IKM has been extensively studied using a number of powerful techniques [2–5,12], and certain similarities have been found [4–6,11,12] between it and the 2CK model [14,15],

$$H_{\rm 2CK} = H_0 + H_{\rm ps} + J_L \vec{S} \cdot \vec{s}_{0L} + J_R \vec{S} \cdot \vec{s}_{0R}, \qquad (2)$$

with $\vec{S}$ a spin-$\frac{1}{2}$ operator for a single impurity, exchange coupled to two independent conduction channels. The physics of the 2CK model is itself immensely rich [15]: the impurity is fully Kondo screened by the more strongly coupled conduction channel below an effective single-channel scale T_K, producing two distinct phases as a function of $(J_L - J_R)$. But when $J_L = J_R$, the frustration inherent when two channels compete to screen the impurity results in "overscreening," and NFL physics results below $T_K^{\rm 2CK}$ [15]. Strikingly, both 2CK and 2IKM have the same fractional residual entropy, $S_{\rm imp} = \frac{1}{2}\ln(2)$.

Conformal field theory (CFT) has been used to describe the critical points of both models [4,16]. In the "unfolded" representation, H_0 is written in terms of left-moving chiral Dirac fermions. The CFTs for each model can be separated into different symmetry sectors. In particular, the $SU(2)_2 \times SU(2)_2 \times U(1)$ flavor, spin, and charge symmetries of the 2CK model [16] and the $U(1) \times U(1) \times SU(2)_2 \times Z_2$ left or right charge, total spin, and Ising symmetries of the 2IKM [3] can be exploited. The 2CK and 2IKM critical fixed point Hamiltonians take the same form as H_0, but with modified boundary conditions that affect only the spin sector of the 2CK model [16] or the Ising sector of the 2IKM [4]. The finite size spectrum (FSS) at the critical point of each model can then be determined [4,16]. In the channel-symmetric case $J_L = J_R$ and for $H_{\rm ps} = 0$, the FSS of the 2CK critical point is characterized by the fractions $0, 1/8, 1/2, 5/8, 1, \ldots$, while for 2IKM a different FSS arises: $0, 3/8, 1/2, 7/8, 1, \ldots$

Despite these apparent differences between the critical FPs of the two models, the 2IKM can be mapped onto an effective 2CK model in special cases [5,6,11]. The key requirement for that mapping is of course the generation of an effective spin-$\frac{1}{2}$ local moment (LM), which can then be overscreened by symmetric coupling to two conduction channels. In the channel-asymmetric limit $J_L \gg J_R$, 2CK critical physics arises via a simple mechanism [6], first involving Kondo screening of the L impurity by the L lead on the single-channel scale T_K^L, followed by second-stage overscreening of the R impurity by the R lead and an effective coupling to the remaining Fermi liquid bath states of the L lead below T_c. An effective 2CK model of form Eq. (2), valid at low energies $T \lesssim T_K^L$, can be derived formally using the approach of Ref. [17], exploiting the Wilson chain representation [18], and effective couplings follow as $\rho J_L^{\rm eff} \sim K/T_K^L$ and $\rho J_R^{\rm eff} \sim [1/\rho J_R - 1/\rho J_L]^{-1}$. The 2CK FP is thus stable when $K = K_c \sim T_K^L \rho J_R^{\rm eff}$, so the low-energy physics of the 2IKM is in this case wholly equivalent to that of the 2CK model.

Importantly, however, the L channel free electrons in the effective 2CK model acquire a $\pi/2$ phase shift due to the first-stage single-channel Kondo screening of the L impurity in the original 2IKM. This is seen clearly in the dynamics of the asymmetric 2IKM. To demonstrate this, and to highlight the basic physical picture, Fig. 1 shows spectra $D\rho_\alpha(\omega) \equiv -\pi\rho\,{\rm Im}[t_\alpha(\omega)]$ vs $|\omega|/D$ with $t_\alpha(\omega)$ the scattering t matrix [19]. Results are obtained from numerical renormalization group (NRG), exploiting all model symmetries, discretizing conduction bands of width $2D$ logarithmically using $\Lambda = 3$, and retaining 8000 states per iteration in each of $z = 3$ interleaved calculations (for a review, see Ref. [18]).

Single-channel Kondo screening of the L impurity by the L lead on the scale of T_K^L is seen directly in the L spectra in the upper panel of Fig. 1: a Kondo resonance, reaching the unitarity limit $D\rho_L = 1$, which has precisely the form of a regular single-channel Kondo (1CK) model [10]. This embodies the $\pi/2$ phase shift in the L channel, but no such feature is observed on this energy scale in the R spectra (lower panel of Fig. 1), indicating that the R impurity is still essentially free. On tuning the interimpurity coupling K closer to the critical point of the 2IKM,

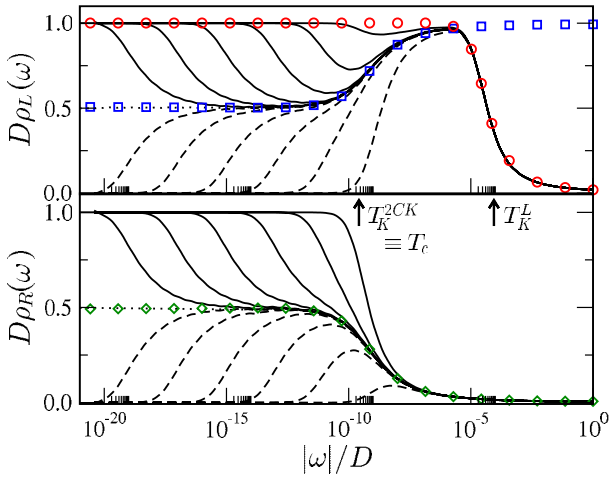

FIG. 1 (color online). Spectra $D\rho_\alpha(\omega)$ versus frequency $|\omega|/D$ for channels $\alpha = L$ and R (upper and lower panels, respectively) for the asymmetric 2IKM with fixed Kondo exchanges $\rho J_L = 0.1$, $\rho J_R = 0.05$, varying interimpurity exchange K (and $H_{\rm ps} = 0$). Plotted using $K = K_c(1 \pm 10^{-n})$ for dashed lines and solid lines, with integer $n = 1 \rightarrow 6$ approaching progressively the critical point $K_c \sim T_K^L \approx 10^{-6} D$ (dotted line). Circles: A 1CK model with $\rho J = \rho J_L$. Diamonds: $D\rho_{\rm 2CK}(\omega)$ for a pure 2CK model with $T_K^{\rm 2CK} = T_c$. Squares: $D\tilde{\rho}_{\rm 2CK}(\omega) = 1 - D\rho_{\rm 2CK}(\omega)$.

the spectra in both channels fold progressively onto the critical spectra. For energies $|\omega|/D \ll T_K^L$, the critical spectrum $D\rho_R(\omega)$ is precisely that of a 2CK model $D\rho_{2\mathrm{CK}}(\omega)$ with $T_K^{2\mathrm{CK}} = T_c$. But the critical spectrum in the left channel is $D\rho_L(\omega) = 1 - D\rho_{2\mathrm{CK}}(\omega)$ [17]. Thus, at the channel-asymmetric critical point [6],

$$D\rho_\alpha(\omega) \overset{|\omega|\ll T_c}{\sim} \tfrac{1}{2} + \alpha\beta\sqrt{|\omega|/T_c}, \tag{3}$$

with $\alpha = \pm 1$ for channel L/R resulting from the additional L channel $\pi/2$ phase shift, and β a constant $\mathcal{O}(1)$.

This phase shift can be included in the 2CK model, Eq. (2), via the potential scattering term H_{ps} (i.e., $V_L \to \infty$ but $V_R = 0$, accompanied also by retuning J_L and J_R to access the critical point). This is equivalent to adding infinite uniform and staggered potential scatterings, which affect, respectively, the charge and flavor sectors of the 2CK model. Modifying the CFT for the critical point of the 2CK model to include this, we find [20] the boundary condition becomes equivalent to that of the 2IKM. The FSS is also naturally affected and is given by [20]

$$E_{2\mathrm{CK}} = \tfrac{1}{8}(Q-a)^2 + \tfrac{1}{4}j(j+1) + \tfrac{1}{4}j_F(j_F+1) - bj_F^z, \tag{4}$$

where Q, j, and j_F are the charge, spin, and flavor quantum numbers. Uniform potential scattering shifts the charge parabolas, while staggered potential scattering biases the flavor sector. The $\pi/2$ phase shift in the L channel corresponds to $a = 1$ and $b = \frac{1}{2}$ [20]. Only certain quantum number combinations are allowed at the critical point, as given by the nontrivial gluing conditions derived in Ref. [16], and which reproduce fully the 2IKM spectrum when used with Eq. (4) (see Fig. 2 of [20]). One remarkable result obtained from our NRG calculations [20] is that the FSS at the critical point of the 2IKM does not depend on channel asymmetry (whence, in particular, the critical point possesses an emergent parity symmetry, irrespective of bare model symmetries). Further, we have shown [20] that the critical point for one model with potential scattering V_L and V_R is equivalent to the critical point of the other model with different potential scattering $\tilde{V}_L$ and $\tilde{V}_R$. The 2IKM and 2CK critical FPs are thus equivalent in the sense that they lie on the same marginal NFL manifold parametrized by H_{ps}.

Conductance line shapes and symmetry.—Full RG flow from the LM FP to the 2CK FP is thus recovered at the critical point of the asymmetric 2IKM. This is manifest [6] in the conductance arising, e.g., when a given channel $\alpha = L/R$ is split into source and drain. At zero bias, it is given exactly [21] in terms of the scattering t matrix (considered for the channel-asymmetric case in Fig. 1) by $G^\alpha_{2\mathrm{IK}}(V_{sd}=0,T)/(2e^2h^{-1}G_0^\alpha) = -\int_{-\infty}^{\infty} d\omega\, \partial f(\omega/T)/\partial\omega D\rho_\alpha(\omega,T)$, with $f(\omega/T)$ the Fermi function, and the impurity-lead coupling parametrized by $G_0^\alpha = 4\Gamma_s^\alpha\Gamma_d^\alpha/(\Gamma_s^\alpha+\Gamma_d^\alpha)^2$, in terms of the $\alpha = L/R$ hybridizations to source (Γ_s^α) and drain (Γ_d^α). Indeed, in the limit $\Gamma_s^\alpha \gg \Gamma_d^\alpha$ (i.e., $G_0^\alpha \ll 1$), the $T = 0$ conductance follows as $\tilde{G}^\alpha_{2\mathrm{IK}}(V_{sd}) = G^\alpha_{2\mathrm{IK}}(V_{sd}, T=0)/(2e^2h^{-1}G_0^\alpha) = D\rho_\alpha(\omega = V_{sd}, T = 0)$, and hence from Eq. (3) one finds at low energies $V_{sd} \ll T_c$,

$$\tilde{G}^{\,\alpha}_{2\mathrm{IK}}(V_{sd}) = \tfrac{1}{2} + \alpha\beta\sqrt{V_{sd}/T_c} + \gamma_\alpha(V_{sd}/T_c) + \cdots, \tag{5}$$

where we include also a term linear in V_{sd}/T_c.

The leading square-root behavior of Eq. (5) has been viewed as the "smoking gun" signature of this 2CK physics [6,22], and was used to identify the critical point in the 2CK experiment of Ref. [13]. But we note that, unlike the 2CK model, the 2IKM does not possess $SU(2)$ flavor symmetry. Since symmetry dictates which operators can act in the vicinity of the critical FP, this is naturally reflected in the asymptotic conductance through the coefficients β and γ_α. Indeed, the full energy dependence of conductance depends on the unstable FPs, whose vying effects on RG flow again depend on symmetry and model parameters. For example, in the usual symmetric 2IKM [Eq. (1) with $J_L = J_R$ and $H_{\mathrm{ps}} = 0$], no incipient LM is formed: there is no intermediate energy window with, e.g., $S_{\mathrm{imp}} = \ln(2)$ entropy, and RG flow proceeds directly to the 2CK FP from the LM $\times$ LM high energy FP describing a pair of free impurities [$S_{\mathrm{imp}} = \ln(4)$].

The effect of parity breaking is explored in Fig. 2, showing NRG results for conductance versus bias V_{sd} at the 2IKM critical point (obtained for $G_0^\alpha \ll 1$, as above). Conductance in the asymmetric limit $J_L \gg J_R$ is

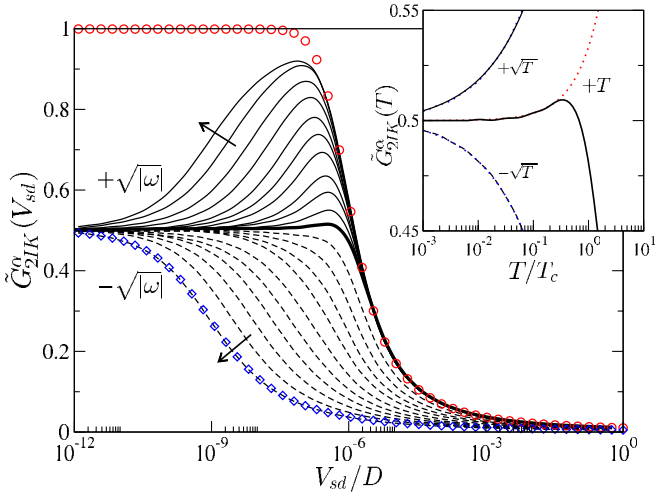

FIG. 2 (color online). $T = 0$ conductance $G^\alpha_{2\mathrm{IK}}/(2e^2h^{-1}G_0^\alpha)$ through channel $\alpha = L$ and R (solid and dashed lines) versus bias V_{sd}/D, at the critical point. Shown for $\rho J_L = 0.075 \geq \rho J_R$, varying $\rho J_R = 0.075 \to 0.05$ in steps of 0.0025, with $K = K_c \sim T_{KL}^{1\mathrm{CK}}$ retuned in each case (and $H_{\mathrm{ps}} = 0$). Thick solid line is the symmetric case $J_L = J_R$; asymmetry $J_L/J_R \geq 1$ increases in direction of arrows. Circle and diamonds: Pure 1CK and 2CK scaling spectra. Inset: Zero-bias conductance versus T/T_c for $J_L/J_R = 1$ and 2 (and $\alpha = L, R$), exhibiting, respectively, leading linear and square-root behavior (dotted lines).

consistent with Ref. [6], and physical expectation as above [see Eq. (5)]. Here, the asymptotic conductance is $\tilde{G}^R_{\rm 2IK}(V_{sd}) \simeq 1 - \tilde{G}^L_{\rm 2IK}(V_{sd}) \equiv \tilde{G}_{\rm 2CK}(V_{sd})$ at low energies $V_{sd} \ll T_K^L$, where $T_K^L \gg T_c \equiv T_K^{\rm 2CK}$ and with $\tilde{G}_{\rm 2CK}(V_{sd})$ the conductance of the standard 2CK model [13,22] (diamonds). Thus, on exchanging $J_R \leftrightarrow J_L$, the coefficient β of Eq. (5) must change sign. But what happens as the asymmetry is decreased? We find the leading square-root contribution in Eq. (5) vanishes (see Fig. 2), as $\beta \sim (J_L - J_R)$, and leading *linear* behavior emerges at the symmetric point $J_L = J_R$ (the same naturally arising as a function of T at zero bias, see Fig. 2 inset). In fact, linear-V_{sd} behavior also emerges as the symmetric point is approached, since the square-root term dominates over a shrinking window $V_{sd}/T_c \ll (\beta/\gamma_\alpha)^2$.

Another striking feature of the conductance in more channel-symmetric situations is the behavior at higher T or energies $\gtrsim T_c \approx T_K^L$. Here the behavior is wholly characteristic of single-impurity, single-channel Kondo physics, as seen by comparison to the circles in Fig. 2.

The absence of square-root behavior in conductance of the symmetric 2IKM is contrary to common belief [6,7], so we now sketch our CFT proof [20]. As pointed out in Refs. [4,6], corrections to the t matrix in the vicinity of the critical point (whose ω dependence displays the same scaling as conductance) are determined from irrelevant boundary operators consistent with symmetry. Two such operators play a role here: $\delta H_1 = c_1 \epsilon'$ and $\delta H_2 = c_2 \vec{J}_{-1} \cdot \vec{\phi}$ (in the notation of Ref. [4]). The operator $\vec{J}_{-1} \cdot \vec{\phi}$ is the leading irrelevant operator of the 2CK FP, whose effect on the t matrix is known [23] to yield the famous square-root behavior. However, $\vec{J}_{-1} \cdot \vec{\phi}$ has *odd* parity in the 2IKM (unlike 2CK), which implies that its coefficient $c_2 \sim (J_L - J_R)$ vanishes in the symmetric limit. In both models, δH_1 does still contribute (c_1 always being finite [4]). One might naively expect ϵ' to behave similarly to $\vec{J}_{-1} \cdot \vec{\phi}$ since they have the same scaling dimension $3/2$. However, the key difference between ϵ' and $\vec{J}_{-1} \cdot \vec{\phi}$ is that only the latter is a Virasoro primary field. Consequently [20], the leading square-root correction to the t matrix from δH_1 vanishes. In the symmetric 2IKM, the leading square-root behavior of conductance thus also vanishes.

Spin-S 2IKM.—Multilevel quantum dots can behave like $S = 1$ impurities [24], and high-spin impurities such as Co ($S = 3/2$) have been manipulated with STM [25]. Thus a natural and pertinent generalization of the 2IKM involves spin-S impurities: the model remains Eq. (1), but $\vec{S}_R$, $\vec{S}_L$ are now spin-S operators.

A QPT must again arise, as follows from the same line of argument as the spin-$\frac{1}{2}$ 2IKM [3]. On tuning K there is a phase-shift discontinuity on going from the local singlet phase for large K to a separated spin-S *underscreened* Kondo phase for small K. The nature of the transition arising at K_c is again clear by considering the asymmetric limit $J_L \gg J_R$. For concreteness consider $S = 1$, although the argument extends easily to higher S. NRG results for the entropy $S_{\rm imp}(T)$ versus T are shown in Fig. 3, together with illustrations highlighting the key physical processes. In 3(a) the impurities are completely decoupled ($K = 0$), with each thus underscreened to a spin-$\frac{1}{2}$ by its attached lead α, on its own single-channel Kondo scale T_K^α [with residual entropy $2\ln(2)$]. For small finite $K < T_K^R$, 3(b), these residual moments form a local singlet state on the scale $T \sim K$, so the residual entropy is quenched. On increasing the interimpurity K further ($T_K^R < K < T_K^L$), the underscreened spin-$\frac{1}{2}$ L impurity and the still unscreened spin-1 R impurity are coupled and form a local doublet state on the scale $T \sim K$. This can then be single-channel Kondo screened by an effective coupling either to the L channel, 3(c), or the R channel, 3(e), and the residual entropy is again quenched. However, L and R effective couplings can become equal on fine-tuning K. This is the single spin-$\frac{1}{2}$ 2CK critical point, 3(d), with residual entropy $\frac{1}{2}\ln(2)$. For large $K \gg T_K^L$, a local interimpurity singlet state arises as expected, 3(f).

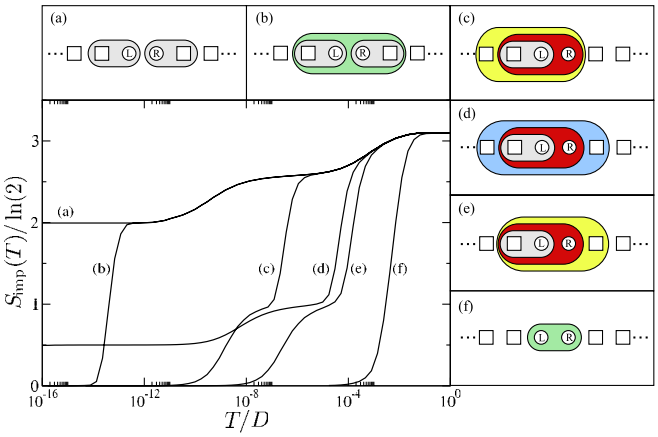

FIG. 3 (color online). Impurity entropy $S_{\rm imp}(T)$ versus T/D for the 2IKM with spin-1 impurities. Plotted for fixed $\rho J_L = 0.15$, $\rho J_R = 0.05$, varying $K/D = 0, 10^{-13}, 3\times10^{-7}$, $K_c \approx 6\times10^{-5}, 2\times10^{-4}$, and 10^{-2} for lines (a)–(f). The corresponding physical processes are illustrated in panels (a)–(f): impurities denoted as circles and conduction band orbitals (in the Wilson chain representation [18]) as squares. For discussion, see text.

Analysis of the finite size spectrum at the critical point shows it to be *identical* to that of the regular spin-$\frac{1}{2}$ 2IKM, independent of asymmetry [20], and is hence that of a 2CK model with additional potential scattering.

Conclusion.—We have shown the critical point of the spin-S 2IKM, including the spin-$\frac{1}{2}$ variant, to be ubiquitously 2CK in nature. However, conductance line shapes measurable in experiment exhibit distinctive behavior depending on underlying symmetries, the low-energy behavior, in particular, evolving from square-root to linear behavior in V_{sd} or T as the channel-symmetric point is approached, and for any spin S.

We thank I. Affleck and T. Quella for insightful input, and acknowledge financial support from the DFG through SFB608 and FOR960 (A. K. M.), the A. v. Humboldt foundation (E. S.), and EPSRC through EP/I032487/1 (D. E. L.).

[1] C. Jayaprakash, H. R. Krishna-murthy, and J. W. Wilkins, Phys. Rev. Lett. **47**, 737 (1981).
[2] B. A. Jones and C. M. Varma, Phys. Rev. Lett. **58**, 843 (1987).
[3] I. Affleck and A. W. W. Ludwig, Phys. Rev. Lett. **68**, 1046 (1992).
[4] I. Affleck, A. W. W. Ludwig, and B. A. Jones, Phys. Rev. B **52**, 9528 (1995).
[5] J. Gan, Phys. Rev. Lett. **74**, 2583 (1995).
[6] G. Zaránd, C.-H. Chung, P. Simon, and M. Vojta, Phys. Rev. Lett. **97**, 166802 (2006).
[7] A. M. Chang and J. C. Chen, Rep. Prog. Phys. **72**, 096501 (2009).
[8] W. G. van der Wiel *et al.*, Rev. Mod. Phys. **75**, 1 (2002).
[9] J. Bork *et al.*, Nature Phys. **7**, 901 (2011).
[10] A. C. Hewson, *The Kondo Problem to Heavy Fermions* (Cambridge University Press, Cambridge, England, 1993).
[11] F. W. Jayatilaka, M. R. Galpin, and D. E. Logan, Phys. Rev. B **84**, 115111 (2011).
[12] E. Sela, A. K. Mitchell, and L. Fritz, Phys. Rev. Lett. **106**, 147202 (2011).
[13] R. M. Potok, I. G. H. Shtrikman, Y. Oreg, and D. Goldhaber-Gordon, Nature (London) **446**, 167 (2007).
[14] P. Nozières and A. Blandin, J. Phys. (Paris) **41**, 193 (1980).
[15] D. L. Cox and A. Zawadowski, Adv. Phys. **47**, 599 (1998).
[16] I. Affleck and A. W. W. Ludwig, Nucl. Phys. **B360**, 641 (1991).
[17] A. K. Mitchell, D. E. Logan, and H. R. Krishnamurthy, Phys. Rev. B **84**, 035119 (2011).
[18] R. Bulla, T. Costi, and T. Pruschke, Rev. Mod. Phys. **80**, 395 (2008).
[19] A. K. Mitchell and D. E. Logan, Phys. Rev. B **81**, 075126 (2010).
[20] See Supplemental Material at http://link.aps.org/supplemental/10.1103/PhysRevLett.108.086405 for detailed derivation of the connection between the critical finite size spectra of 2CK and 2IKM, CFT analysis of the t matrix for the symmetric 2IKM, and further supporting numerical renormalization group calculations.
[21] Y. Meir and N. S. Wingreen, Phys. Rev. Lett. **68**, 2512 (1992).
[22] M. Pustilnik, L. Borda, L. I. Glazman, and J. von Delft, Phys. Rev. B **69**, 115316 (2004).
[23] I. Affleck and A. W. W. Ludwig, Phys. Rev. B **48**, 7297 (1993).
[24] D. E. Logan, C. J. Wright, and M. R. Galpin, Phys. Rev. B **80**, 125117 (2009).
[25] A. F. Otte *et al.*, Nature Phys. **4**, 847 (2008).